An Improved Camera Identification Method based on the Texture Complexity and the Image Restoration

[1]Kazuya Matsushita and [2]Hitoshi Kitazawa

[1,2]Department of Electrical and Electronic Engineering, Tokyo University of Agriculture and Technology, Tokyo, Japan
[1]50008645228@st.tuat.ac.jp, [2]kitazawa@cc.tuat.ac.jp

Abstract

The identification of source camera is useful to improve the capability of evidence in the digital image such as distinguish the photographer taking illegal images and adopting digital images as evidence of crime. Lukáš, et al. showed the method for source camera identification based on the correlation of PNU (pixel non-uniformity) noise. However, the wavelet-based denoising filter for suppressing the random noise reduces the accuracy of camera identification. It is caused by the fact that the denoising filter diffuses the edge and makes the PNU noise less pronounced. Moreover, it is difficult to extract PNU noise from the images taken by cameras which are equipped with the image improvement functions such as motion blur correction, contrast enhancement, and noise reduction. In this paper, we propose a method for improving the camera identification accuracy by selecting pixels based on the texture complexity. We also propose a method for improving the identification accuracy by applying the image restoration method.

Keywords: *PNU Noise, Camera Identification, Image Restoration.*

1. Introduction

Digital images and videos do not have the reliance of contents because the digital images can easily be tampered. Therefore, source camera identification is useful in image forensics. Several methods for camera identification have already been proposed. Lukáš, et al. proposed the method which identifies the camera by the correlation of the pixel-non-uniformity (PNU) noise [1]. The PNU noise is extracted by wavelet-based denoising filter [2]. However, the filtering process strongly influences the pixel values around the edges in the image. Therefore, the identification accuracy is reduced if the image includes complex textured area. For solving this problem, we propose a method to select pixels used for identification according to the texture complexity. In addition, we show that the camera identification accuracy is reduced by the image processing engine such as motion blur correction, contrast enhancement, and noise reduction. We also propose a method for improving the identification accuracy by the image restoration method.

The rest of this paper is organized as follows: In Section 2, we briefly explain the outline of the camera identification method proposed by Lukáš, et al. In Section 3, we describe our improvement method for camera identification by selecting pixels based on the texture complexity. In Section 4, we propose to apply the image restoration method for extracting the PNU noise from the images modified by the image processing engine. Finally, the paper is concluded in Section 5.

2. Camera identification method based on the sensor pattern noise

In this section, we briefly explain the camera identification method based on the sensor pattern noise proposed by Lukáš, et al [1]. The processing flow of the method is shown in Fig. 1.

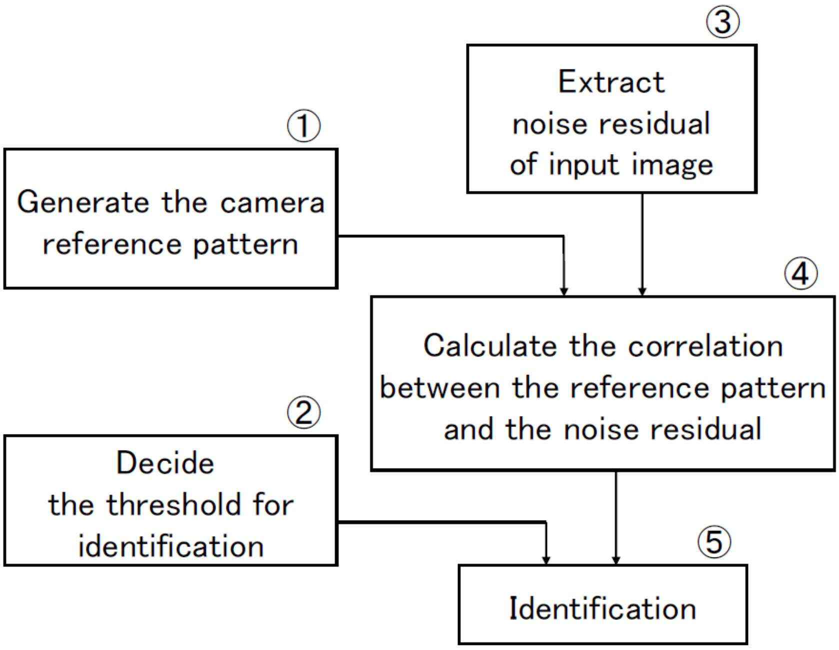

Figure 1. Camera identification flow

2.1. Noise of digital images

The digital image will still exhibit small differences in intensity between individual pixels even if the imaging sensor takes a picture of evenly illuminated scene. This is partly because of random noise, and a partly because of pattern noise. The random noise has property that the signal changes time-wise. On the other hand, the pattern noise stays approximately the same if multiple pictures of the exact same scene are taken. Therefore it is a deterministic component. Due to this property, the pattern noise is present in every image taken by the sensor and thus can be used for camera identification.

2.2. Pattern noise

Pattern noise is classified into FPN (fixed pattern noise) and PRNU (photo-response non-uniformity noise) as shown in Fig. 2 [1].

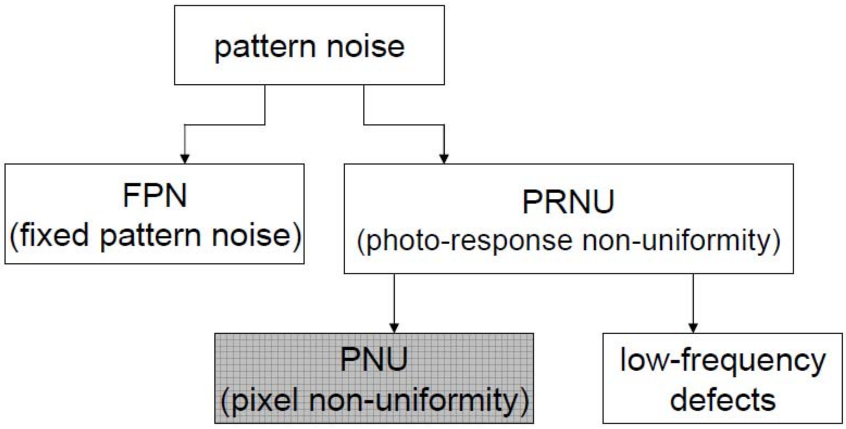

Figure 2. Classification of pattern noise

The fixed pattern noise is caused by dark currents when the sensor array is not exposed to light. In general, this noise is suppressed automatically by subtracting a dark frame from every image. Therefore, it can't be used for camera identification. The photo-response non-uniformity noise is classified into PNU (pixel non-uniformity) noise and low-frequency defects. Since PNU noise is caused from the difference of image sensor sensitivities, it is useful for identification of source camera. The low-frequency defects are caused from vignetting and others.

2.3. Noise residual

Because the PNU noise cannot be observed directly, an approximation of the PNU noise called noise residual is used. Let *P(k)* and *F* be an image *k* and a denoising filter, respectively. Then the noise residual *n(k)* is given by Eq. (1).

$$n^{(k)} = p^{(k)} - F(p^{(k)}). \tag{1}$$

2.4. Reference pattern

Noise residual, which is a noise component of an image, contains not only PNU noise but also much random noise. In addition, the scene contents from the image influence the *n(k)* and they must be suppressed. Therefore, the reference pattern is calculated by averaging multiple noise residual made from uniformly illuminated images such as blue sky.

2.5. Calculation of correlation

For deciding if the image p was taken by camera C, correlation between the noise residual n of image p and the reference pattern P_c is calculated by Eq. (2).

$$\rho_c(p) = corr(n, P_c) = \frac{(n - \bar{n}) \cdot (P_c - \bar{P}_c)}{\|n - \bar{n}\| \|P_c - \bar{P}_c\|}. \tag{2}$$

Where $\bar{n}$ and $\bar{P}_c$ denote the average value of n and P_c, respectively.

2.6. Detection by correlation

Suppose that image p is taken by camera C and image q is taken by another camera. The false acceptance rate (FAR) is the probability of miss identification which means the image q is regarded as a picture taken by camera C. The false rejection rate (FRR) is the probability of another miss identification representing the situation that the image p is not regarded as taken by camera C (actually, it is). The threshold of the correlation in the camera identification method should be determined by the required identification accuracy. In the court, low FAR is required to keep reliance of the identification method. In this paper, the FAR is set to 10^{-3}. Under this condition, it is required to reduce FRR as small as possible. The identification threshold is determined by approximating the distribution of ρ by a Gaussian function.

3. Texture complexity and reliability of identification

3.1. Detection by correlation

The Wavelet-based filter used for denoising spread the edge of the image. Therefore, the noise residual made from complex textured image includes many disturbing signals for identification as shown in Fig. 3.

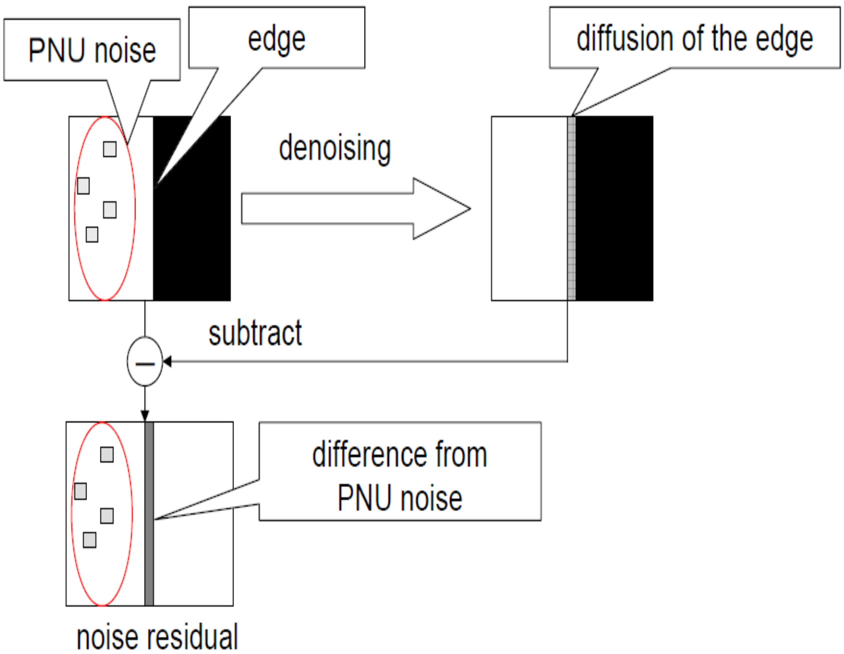

Figure 3. Influence of an edge to the noise residual

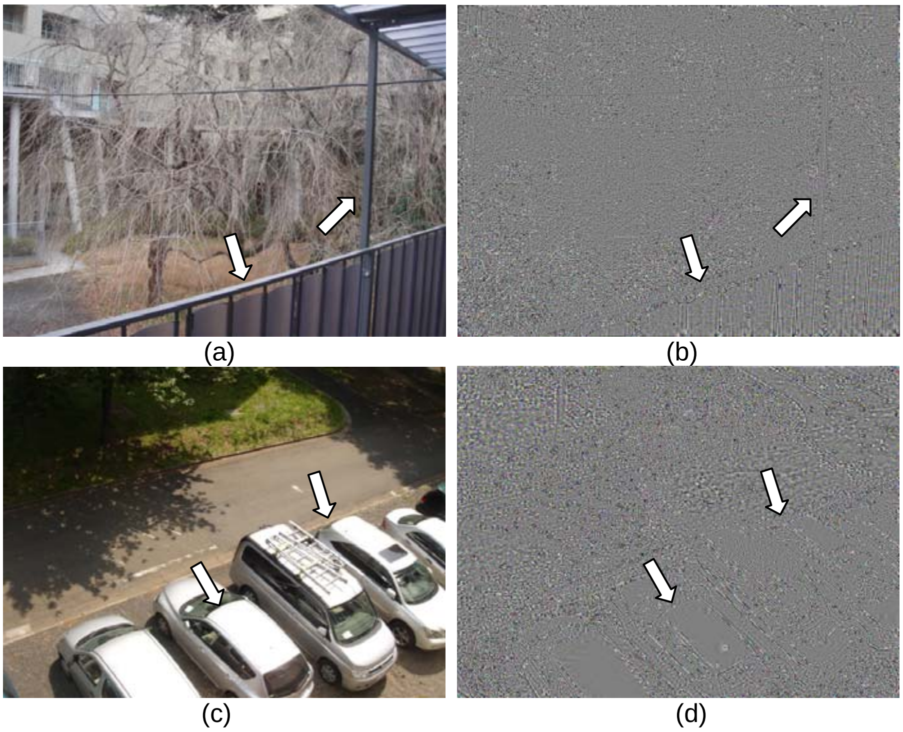

Figure 4. Example of influence from edges in the image

We show some examples of the noise residual for complex textured images. Figures 4 (b) and 4 (d) are the noise residual of Figs. 4 (a) and 4 (c), respectively. Figures 4 (b) and 4 (d) are generated from $n^{(k)}$ by multiplying 16 and adding 128. It can be observed that there is heavy effect around the edges of the original image.

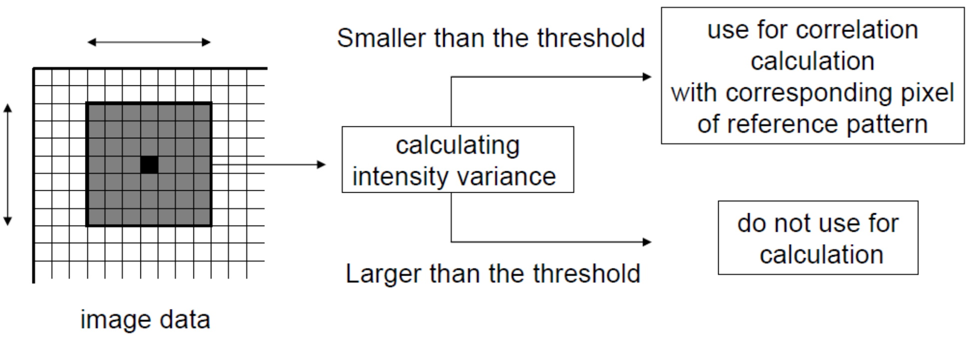

Figure 5. Identification with eliminating complex textured area

$$\sigma^2 = \frac{1}{N}\sum_{i=1}^{N}(x_i - \bar{x})^2. \tag{3}$$

3.2. Pixel selection by intensity variance

In order to improve the identification accuracy, we need to avoid the influence caused by the edges. Therefore, we select the pixels used for calculating the correlation in Eq. (2) by the complexity of edges around a pixel. In this study, we use variance of intensity as indicating the criterion of texture complexity as shown in Fig. 5. The variance σ^2 is calculated by the intensity of pixels inside the square area around the pixel as shown in Eq. (3), where N means the number of pixels inside the area, x_i means intensity of pixel i, and $\bar{x}$ means average intensity in the area. Then if the variance is smaller than a predefined threshold we use the center pixel for calculating correlation. If the variance is larger than the threshold we do not use it for calculating. We eliminate the influence of edge by this procedure.

3.3. Experimental results of pixel selection

We replayed experiment using six cameras for confirming accuracy of camera identification method based on PNU noise [1]. The wavelet-based filter [2] is used for denoising as same as [1]. We decided the threshold and calculated the FRR of each camera. The image size was 640×480. The functions of flash and digital zoom were set to off. Reference pattern was generated using about 100 blue sky pictures. The threshold FAR=10^{-3} was decided from about 500 images taken by other cameras. FRR was calculated from about 100 images taken by each camera.

Table 1. Accuracy of camera identification

candidate cameras	threshold	FRR	approximation FRR
Canon VB-C10 306	0.0620	0.9041	0.9455
Canon VB-C10 320	0.0709	0.3378	0.2609
FUJIFILM FinePix30i	0.0462	0.0811	0.1087
FUJIFILM FinePix2800Z	0.0481	0.1126	0.1586
Panasonic FX150	0.0394	0.5952	0.4369
CASIO EX-F1 JPEG97	0.0496	0.0588	0.0794

Table 2. Experimental result applied pixel selection

candidate cameras	threshold	FRR	approximation FRR
VB-C10 306	0.0216	0.0000	2.753×10^{-6}
VB-C10 320	0.0248	0.0000	5.478×10^{-8}
FinePix30i	0.0127	0.0000	0.0237
FinePix2800Z	0.0102	0.0000	0.0023
FX150	0.0254	0.4048	0.2921
EX-F1	0.0202	0.0294	0.0459

Figure 6. Discarded area by pixel selection in Fig. 4 (a)

Figure 7. Discarded area by pixel selection in Fig. 4 (c)

Table 1 shows the experimental results by the original method proposed by Lukáš, et al. In table 1, the FRR of camera C is calculated from Eq. (4).

$$1-\frac{\text{(number of identified images to be taken by camera C)}}{\text{(number of images taken by camera C)}}. \quad (4)$$

The approximation FRR is calculated from probability distribution based on Gaussian approximation of correlation coefficients. The FRR is quite large in table 1. Table 2 shows the results of identification using proposed pixel selection. The area size for variance calculation is 7×7. The threshold of variance is σ^2=25. The other settings are the same as the previous experiment.

From table 2, it can be seen that approximation FRR has been improved largely compared to that in table 1. An example of discarded area for identification is shown in Figs. 6 and 7. Red colored pixels are discarded.

4. Improvement by image restoration

4.1. Effect of image processing engine for identification accuracy

In table 2, FX150's FRR has not been improved significantly. FX150 is newer than other cameras, and it is equipped by some image processing function such as noise reduction and contrast enhancement. In order to check if the PNU noise is eliminated in a new camera or it is varied by some image processing engine, we compared the identification accuracy between the RAW data and the JPEG data taken from the same scene. The results are shown in table 3.

Table 3. The result of comparison raw data with JPEG data

camera type and image format	threshold	FRR	identified images ／all images	approximation FRR
Panasonic FX150(RAW)	0.0087	0.0714	78 ／ 84	0.1051
Panasonic FX150(JPEG)	0.0254	0.4048	50 ／ 84	0.2921

From this result, we can expect that the camera identification accuracy has been reduced by the image processing engine as shown in Fig. 8.

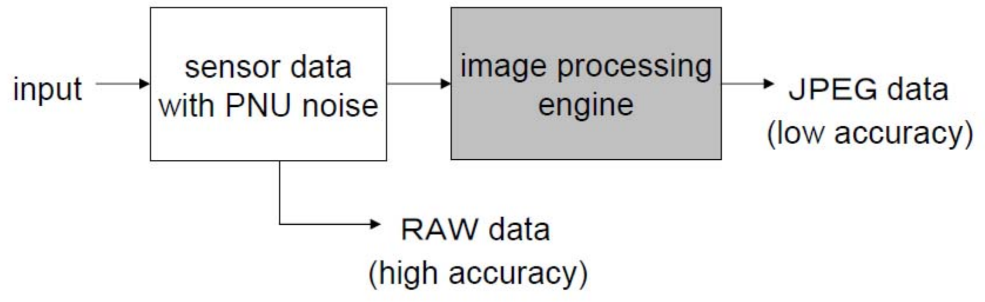

Figure 8. Reduction of identification accuracy by image processing engine

4.2. Improve identification accuracy by image restoration

From the estimation at the previous section, we expect that reverse transformation of process in the image processing engine can improve the identification accuracy. Therefore, we apply image restoration method. Assume that *f(x,y)* is sensor output RAW data, *h(x,y)* is function of image processing engine, and *g(x,y)* is the camera output. *g(x,y)* is expressed as Eq. (5). Equation (6) is led from Eq. (5) by Fourier transform.

$$g(x,y) = f(x,y) * h(x,y) \tag{5}$$

$$G(u,v) = F(u,v)H(u,v) \tag{6}$$

$$F(u,v) = G(u,v)/H(u,v) \tag{7}$$

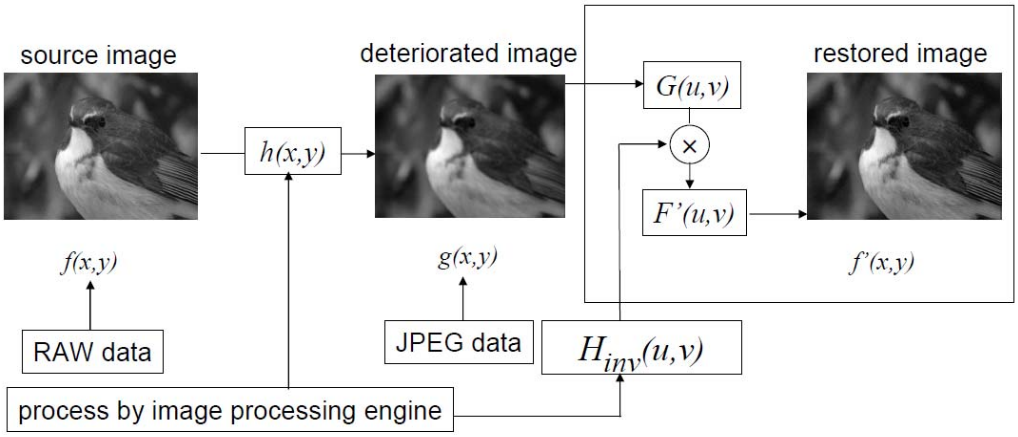

Figure 8. Reduction in effect of image processing by the image restoration method

Source signal *f(x,y)* can be restored by inverse Fourier transform of *F(u,v)* Eq. (7). This procedure is shown in Fig. 8.

4.3. Restoration by point spread function

Since the image processing technology in the camera is considered proprietary, most camera manufacturers do not provide details of the *h(x,y)*. We thus apply the blind signal processing technology to restore the PNU noise. We tested two point spread functions (PSF) as *h(x,y)*: Gaussian function and low-pass type function. We obtained better result using low-pass type function in Eq. (8).

In addition, we applied the Wiener filter shown in Eq. (9), because the restored image calculated from Eq. (7) can be a value of infinity in the case of $H(u,v)=0$, and the PNU noise is disturbed. In Eq. (9), N is a noise component and $|N(u,v)|^2/|F(u,v)|^2$ is treated as a parameter Γ.

$$h(x,y) = \begin{cases} \dfrac{1}{2\pi R^2} & if \quad x^2 + y^2 \le R^2 \\ 0 & if \quad x^2 + y^2 > R^2 \end{cases} \tag{8}$$

$$M(u,v) = \frac{1}{H(u,v)} \frac{|H(u,v)|^2}{|H(u,v)|^2 + |N(u,v)|^2 / |F(u,v)|^2} \tag{9}$$

4.4. Experimental results and discussion

We show the experimental results of FX150 applied image restoration method given by Eqs. (8) and (9). We repeated the experiment with changing R and Γ variously as shown in table 4. The highest accuracy of identification is obtained when R=1 and Γ=0.000025. Within the tested 84 images, the number of false rejected images is reduced from 34 to 21. We expect this improvement of identification accuracy by the image restoration method can be applied to other cameras.

Table 4. Experimental Result Applied Eq. (8) as PSF

R	Γ	threshold	identified images /all images	FRR	approximation FRR
not applying		0.0254	50 / 84	0.4048	0.2921
1	0.01	0.0357	32 / 84	0.6190	0.3926
1	0.001	0.0344	33 / 84	0.6071	0.3567
1	0.0005	0.0301	36 / 84	0.5714	0.3300
1	0.0001	0.0205	57 / 84	0.3214	0.2677
1	0.000075	0.0193	59 / 84	0.2976	0.2570
1	0.00005	0.0179	61 / 84	0.2738	0.2439
1	0.00003	0.0163	61 / 84	0.2738	0.2275
1	0.000025	0.0160	63 / 84	0.2500	0.2258
1	0.00002	0.0160	63 / 84	0.2500	0.2271
1	0.00001	0.0163	62 / 84	0.2619	0.2446
2	0.01	0.0410	39 / 84	0.5357	0.4113
2	0.001	0.0361	35 / 84	0.5833	0.4353
3	0.01	0.0450	41 / 84	0.5119	0.4383

5. Conclusions and future works

In this paper, we have shown the improved camera identification method. The identification accuracy is improved by selecting pixels used for correlation calculation according to the texture complexity. And the identification accuracy is also improved by the image restoration which restores the PNU noise varied by the image processing engine. The systematic method to correctly estimate the restoration function is left to the future work.

References

[1] J Lukas, et al. “Digital Camera Identification from Sensor Pattern Noise″, IEEE Trans. IFS, June 2006

[2] Mihcak M.K.,et al.: ″Spatially adaptive statistical modeling of wavelet image coefficients and its application to denoising,″ in Proc. IEEE Int. Conf. Acoustics, Speech, and Signal Processing, Mar. 1999

Authors

Kazuya Matsushita received the B.S. degrees in electrical and electronic engineering from Tokyo University of Agriculture and Technology, Japan, in 2008. He is currently a M.S. student of Department of Electrical and Electronic Engineering at the Tokyo University of Agriculture and Technology. His research interests are in Image Processing and Digital Image Forensic.

Hitoshi Kitazawa received his B.S, M.S and Ph.D. degrees in electronic engineering from Tokyo Institute of Technology, Tokyo Japan, in 1974, 1976 and 1979, respectively. He joined the Electrical Communication Laboratories, Nippon Telegraph and Telephone Corporation(NTT), in 1979. Since 2002, he is a professor at Tokyo University of Agriculture and Technology. His research interests are in VLSI CAD algorithm, Computer Graphics and Image Processing. He is a member of IPSJ, IEICE and IEEE.